Differentiation of glioblastoma and primary central nervous system lymphomas using multiparametric diffusion and perfusion magnetic resonance imaging

NGUYEN DUY HUNG[1,2], NGUYEN NGOC ANH[1], NGUYEN DINH MINH[2], DANG KHANH HUYEN[1] and NGUYEN MINH DUC[3]

[1]Department of Radiology, Hanoi Medical University; [2]Department of Radiology, Viet Duc Hospital, Hanoi 100000; [3]Department of Radiology, Pham Ngoc Thach University of Medicine, Ho Chi Minh 700000, Vietnam

Received May 16, 2023; Accepted September 13, 2023

DOI: 10.3892/br.2023.1664

Abstract. The present study aimed to determine whether combining diffusion-weighted (DWI) and dynamic susceptibility contrast-enhanced perfusion-weighted (DSC-PWI) magnetic resonance imaging (MRI) could differentiate between primary central nervous system lymphoma (PCNSL) and glioblastoma (GBM). The present retrospective study evaluated 45 patients with histologically confirmed brain tumors, of which 18 had PCNSLs and 27 had GBMs. All patients underwent conventional, DWI, and DSC-PWI MRIs before the surgical removal of the lesion or stereotactic biopsy. The solid tumor component, peritumoral edema, and abnormal white matter were measured in three regions of interest to evaluate relative cerebral blood volume (rCBV), apparent diffusion coefficient (ADC) and DWI. In conventional MRI, there were significant differences in tumor numbers, tumor enhancement type, tumor necrosis, hemorrhage and open-ring sign between GBM and PCNSL. Solid tumor ADC and rCBV values (ADCt and rCBVt, respectively) and their ratios with abnormal white matter amounts were significantly higher in GBM cases than in PCNSL cases ($P<0.05$). The rCBV value for peritumoral edema (rCBVe) and its ratio with abnormal white matter amount (rCBVe/n) were significantly higher in GBM cases than in PCNSL cases ($P<0.05$). However, ADC values did not differ significantly for peritumoral edema. DWI values did not differ significantly. Combining rCBVt and rCBVe/n provided a perfect area under the receiver operating characteristic curve of 1.00, with 100% sensitivity and 100% specificity for distinguishing GBM from PCNSL. In the results of the present study, the major criterion in the decision-making process distinguishing PCNSL from GBM was the combined rCBVt and rCBVe/n parameter. A minor criterion was the ADCt value of the lesion.

Correspondence to: Dr Nguyen Minh Duc, Department of Radiology, Pham Ngoc Thach University of Medicine, 2 Duong Quang Trung Ward 12 District 10, Ho Chi Minh 700000, Vietnam
E-mail: bsnguyenminhduc@pnt.edu.vn

Key words: diffusion-weighted imaging, perfusion-weighted imaging, lymphoma, glioblastoma

Introduction

Glioblastoma (GBM) is defined by The World Health Organization (WHO) as a grade 4 tumor. It is the most common central nervous system (CNS) malignant tumor, accounting for almost 80% of all primary malignant brain tumors and 50% of all gliomas in all age groups (1). Its original name, GBM multiforme, comes from the historical observation that these tumors can take various forms and appearances, both grossly and microscopically. Notably, 'multiforme' was dropped from its name in the 2016 WHO classification system, which refers to these tumors as GBM instead. However, GBM remains its widely used acronym (2).

The incidence of primary CNS lymphoma (PCNSL), an extra-nodal form of non-Hodgkin lymphoma representing 5% of all brain tumors, has been increasing due to population aging and imaging modality advancements (3,4). The strongest known risk factors for PCNSL is immunodeficiency, and PCNSL is the most common brain tumor in this population (4,5). Multiple studies have suggested that the immune system has an important regulatory role against malignant lymphoproliferative diseases and natural killer (NK) cells serve as a crucial first line of defense against tumors. The dysfunction of NK cells, as well as increased spontaneous lactate dehydrogenase release activity of peripheral blood mononuclear cells is one of the main prognostic factors for lymphomas patients (5,6). Preoperative differentiation of PCNSLs and GBMs is crucial because their treatment strategies and prognosis differ substantially. In patients with GBM, the treatment of choice is gross total resection followed by radiation therapy and chemotherapy (1). By contrast, patients with PCNSL usually undergo stereotactic biopsy followed by high-dose methotrexate-based chemotherapy (7). While histopathological classification remains the gold standard for diagnosis (4,8), this invasive procedure has drawbacks, such as brain edema, hemorrhage, infection and seizure (9). In addition, ~10% of diagnoses are incorrect because the tiny amounts of

tissue obtained by stereotactic biopsy may be insufficient for a correct diagnosis (10). These issues have led to a demand for reliable preoperative differentiation methods. Therefore, over recent decades, new non-invasive imaging techniques have been developed that improve diagnosis, including magnetic resonance imaging (MRI).

Conventional MRI sequences can differentiate most patients because PCNSLs in immunocompetent patients usually appear as homogeneous enhancements on contrast-enhanced T1-weighted (T1W) MRI images, while GBMs usually appear as heterogeneous enhancements with necrotic, hemorrhagic areas. However, this pattern is unreliable because atypical, solid-enhancing GBMs without visible necrosis can mimic typical PCNSLs (11). Similarly, atypical PCNSLs with visible necrosis in immunocompromised patients may mimic typical GBMs. Advanced MRI techniques, such as diffusion-weighted imaging (DWI) and dynamic susceptibility contrast-enhanced perfusion-weighted imaging (DSC-PWI), provide useful physiologic information facilitating the precise evaluation of brain masses to improve the differential diagnosis of GBMs and PCNSLs (12).

DWI is a sensitive tool that quantifies physiologic alterations in water diffusion that can be measured as the apparent diffusion coefficient (ADC). Highly cellular tumors show areas of restricted diffusion with low ADCs (13). DSC-PWI provides information on cerebral physiology at the capillary level (microvasculature) and cerebral blood volume (CBV) maps. Its relative CBV (rCBV) parameter correlates with tumor vascularity and is elevated in tumors with high pathologic neoangiogenesis, such as GBMs (14).

Previous studies have shown that the minimum ADC from DWI and the rCBV from DSC-PWI are the most important hemodynamic parameters for differentially diagnosing GBMs and PCNSLs (15). However, numerous studies have discussed only assessments of tumor cores (3,16-20), with peritumoral regions less frequently evaluated (15,21). To the best of our knowledge, very few studies have evaluated usefulness of multiparametric DSC-PWI and DWI of tumor core and peritumoral zone in the preoperative differentiation of GBMs and PCNSLs. Therefore, the present study not only referred to this issue but also aimed to compare different perfusion and diffusion parameters to identify those with the highest accuracy in distinguishing GBMs and PCNSLs.

Materials and methods

Patient selection. Patients diagnosed with GBM or PCNSL based on the 2021 WHO histopathologic criteria (22) between January 2019 and December 2022, were chosen retrospectively by inspecting the medical records and radiology information systems at Viet Duc Hospital (Hanoi, Vietnam). The present study population was comprised of 45 patients with histologically confirmed tumors, of which 18 had PCNSLs and 27 had GBMs. All patients underwent 3 Tesla MRIs with conventional, DWI, and DSC-PWI sequences before lesion removal or stereotactic biopsy. The present study was approved (approval no. 4096/QD-ĐHYHN; date: September 30, 2022) by Hanoi Medical University Institutional Ethical Review Board (Hanoi, Vietnam) and conducted according to the ethical standards of the 1964 Declaration of Helsinki and its later amendments. The requirement for patient or guardian consent was waived because the present study was retrospective and its data were anonymized. Clinicopathological characteristics of patients (including sex and age distribution) are provided in Table I.

MRI methods. All MRI examinations were performed using a 3 Tesla MRI system (SIGNA Pioneer; GE Healthcare) with a head coil. The same imaging protocol was used for all patients. The conventional MRI included T1W spin-echo (T1 SE) imaging before and after contrast enhancement for multi-planar reconstructed imaging, transverse fluid-attenuated inversion recovery (FLAIR) imaging, and transverse T2-weighted (T2W) gradient-echo (T2 GE) imaging. Patients were not permitted to use steroids during the examination period.

DWI was performed in the transverse plane using a spin-echo planar sequence before contrast-enhanced T1W imaging. ADC maps were constructed on a per-pixel basis.

The transverse DSC-PWI was acquired using a single-shot gradient-echo echo-planar sequence during which gadoteric acid (Dotarem) at 0.1 mmol/kg body weight was injected intravenously at 5 ml/s with a power injector (Medrad Spectris Solaris EP). Following the contrast agent injection, a 20 ml saline bolus was injected at the same rate. No contrast agent was administered before DSC-PWI. The commercially available built-in software calculated rCBV from the DSC-PWI data. The detailed sequence parameters are provided in Table II.

Image analysis. To assess the brain tumors based on imaging, surgical, and histologic data, MR examinations were conducted using a GE SIGNA Pioneer 3.0 Tesla (GE Healthcare) and the entire MRI scan series were evaluated on a Picture Archiving and Communication System workstation 4.7. One radiologist with >10 years of neurological experience who was blinded to the histopathological results created three circular regions of interest (ROIs) on the solid tumor component, peritumoral edema, and abnormal white matter based on T1W pre- and post-contrast, T2 GE, and FLAIR images. The largest lesion was measured for patients with multifocal tumors. The first ROI (predefined size: 30 mm^2) was placed into the visually perceived lowest ADC, highest DWI, and rCBV portions of each tumor while still within the solid tumor component (which had the strongest enhancement on T1W post-contrast images) but avoiding apparent necrotic, hemorrhagic, calcified, or cystic areas or blood vessels that may influence ADC, DWI, and rCBV values, as described by Kickingereder *et al* (12). Other ROIs of the same size were placed in the peritumoral edema (which appears as hyperintensity in FLAIR and T2W images without contrast) and the contra-lateral unaffected white matter (Figs. 1 and 2). In the peritumoral edema, since each edematous location may show varying ADC values, the ROIs were placed in the most proximal location near the enhanced tumor for measurement based on the findings of Ko *et al* (21). The minimum ADC, mean DWI and relative rCBV values were calculated and analyzed in each lesion. To minimize variances in their values in individual patients, ratios were calculated by dividing the value from an ROI in the solid tumor component or peritumoral edema by the value from an ROI in the normal-appearing white matter.

Table I. Patient characteristics and the conventional MRI features of GBMs and PCNSLs.

Characteristics	GBM (n=27)	PCNSL (n=18)	P-value
Age, years [Mean ± SD (range)]	59.04±11.12 (32-76)	59.50±14.16 (18-75)	0.702[b]
n (%)			0.320[a]
<44	3 (11.1)	2 (11.1)	
44-60	10 (37.0)	3 (16.7)	
>60	14 (51.9)	13 (72.2)	
Sex, n (%)			0.714[a]
Male	15 (44.4)	9 (50.0)	
Female	12 (55.6)	9 (50.0)	
Sex ratio (male/female)	5/4	1/1	
Tumor location, n (%)			
Supratentorial	27 (100)	16 (88.9)	0.155[a]
Infratentorial	0 (0)	1 (5.6)	
Both	0 (0)	1 (5.6)	
Corpus callosum	6 (22.2)	3 (16.7)	0.648[a]
Basal ganglia	4 (14.8)	5 (27.8)	0.287[a]
Thalamus	3 (11.1)	5 (27.8)	0.235[a]
Periventricular	11 (40.7)	5 (27.8)	0.373[a]
Brainstem	0 (0)	2 (11.1)	0.155[a]
Quantity, n (%)			0.004[a]
Unifocal	23 (85.2)	8 (44.4)	
Multifocal	4 (14.8)	10 (55.6)	
Tumor margin, n (%)			1.000[a]
Smooth	1 (3.7)	0 (0)	
Irregular	26 (96.3)	18 (100)	
Tumor necrosis, n (%)			<0.001[a]
Yes	27 (100)	3 (16.7)	
No	0 (0)	15 (83.3)	
Tumor hemorrhage, n (%)			<0.001[a]
Yes	23 (85.2)	3 (16.7)	
No	4 (14.8)	15 (83.3)	
Tumor enhancement, n (%)			
Homogeneous	0 (0)	14 (77.8)	<0.001[a]
Heterogeneous	27 (100)	4 (22.2)	
Low	2 (7.4)	0 (0)	0.509[a]
High	25 (92.6)	18 (100)	
Notch sign	0 (0)	0 (0)	0.001[a]
Open-ring sign	0 (0)	6 (33.3)	
Butterfly sign	3 (11.1)	0 (0)	
Peritumoral edema, n (%)			0.844[a]
Grade 0	0 (0	0 (0%)	
Grade 1	5 (18.5)	2 (11.1)	
Grade 2	13 (48.1)	9 (50.0)	
Grade 3	9 (33.3)	7 (38.9)	

GBM, glioblastoma; PCNSL, primary central nervous system lymphoma; a, χ^2 test; b, Mann-Whitney U test. Edema in MRI scans appears as a region of increased T2 signal intensity outside the gadolinium-enhanced area. Edemas measured on T2 images were categorized into three grades: Grade I, an edema volume less than the tumor volume; Grade II, an edema volume ~equal to the tumor volume (Fig. 1C and D); Grade III, an edema volume greater than the tumor volume (Fig. 2C and D). Tumor enhancement was categorized into two groups: low, the foci's increased signal was lower than that of large blood vessels; high, the foci's increased signal was similar to that of large blood vessels.

Table II. Conventional and advanced MRI sequence parameters.

Sequence	Plane	TR (ms)	TE (ms)	Thickness (mm)	Matrix	FOV	Other
FLAIR	Axial	8,500	117	5	184x256	240x240	IR (2500 ms)
T2 TSE	Axial, coronal	2,500	100	5	360x288	220x220	
T2*/SWI	Axial	360	10	5			μ
DWI	Axial	5,202	78	5		230x240	
T1 SE	Axial, sagittal	2,325	24	5	240x240	300x224	
T1 SE CE+	Axial, sagittal	2,325	24	5	240x240	300x244	α
DSC-MRI	GRE EPI	1,250	45	5	88x87	338x240	β

TR, repetition time; TE, echo time; FOV, field of view; FLAIR, fluid-attenuated inversion recovery; IR, inversion time; T2 TSE, T2-weighted turbo spin-echo; SWI, susceptibility-weighted imaging; T1 SE, T1-weighted spin-echo; CE+, contrast enhancement; DSC-MRI, dynamic susceptibility contrast perfusion magnetic resonance imaging (performed using the dynamic T2*-weighted GRE EPI); GRE EPI, gradient-recalled echo-planar imaging; μ, optimal sequence (T2* or SWI) for each patient; α, intravenous injection of contrast agent [gadolinium-diethylenetriamine pentaacetate (DTPA) at 1 ml/kg with an injection rate of 5 ml/s]; β, performed before T1-SE CE+ during the first pass of an intravenous bolus injection of contrast agent (gadolinium-DTPA at 1 ml/kg with an injection rate of 5 ml/s) using 40 acquisition scans with a voxel size of 2.5x2.5x5 mm.

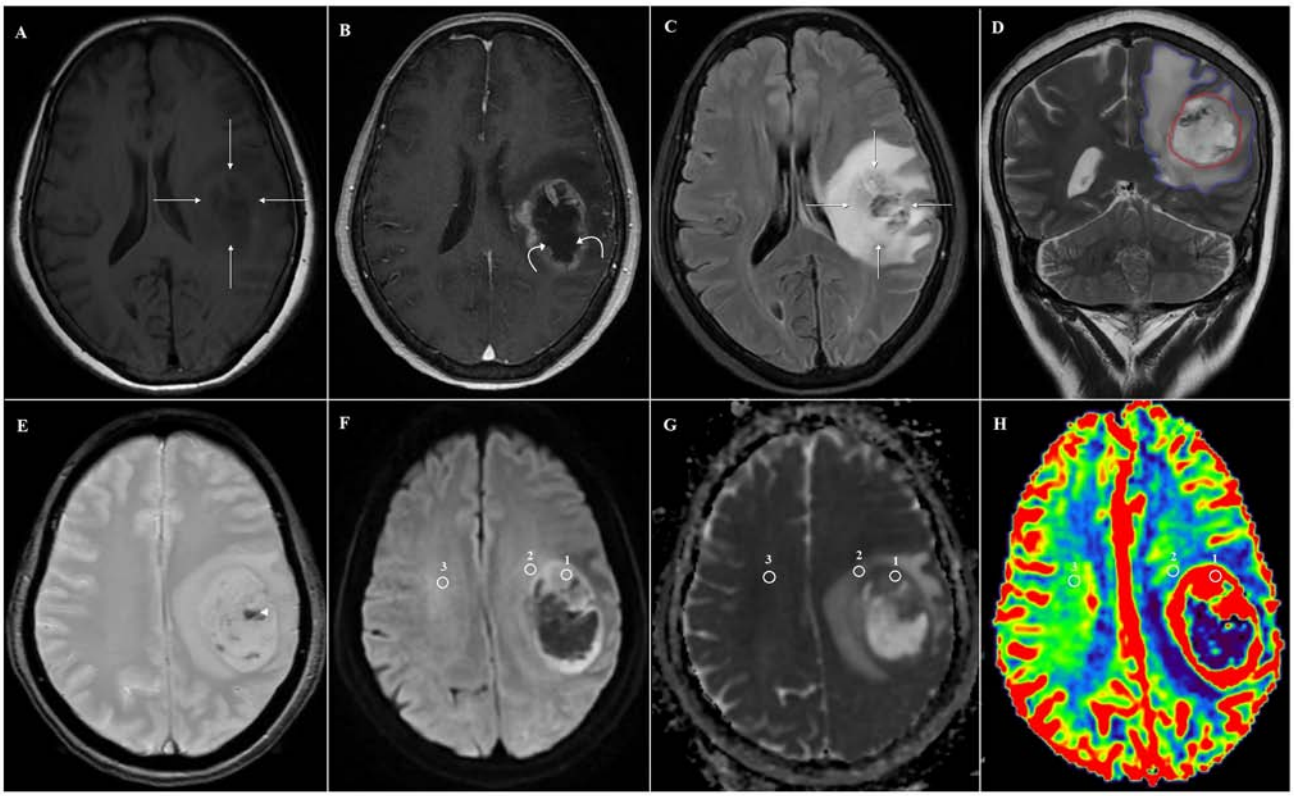

Figure 1. A 61-year-old woman with a GBM. (A) The MRI shows a mass (straight arrows) in the left frontal lobe. A comparison of (A) pre- and (B) post-contrast T1W images shows a heterogeneously enhanced tumor with central necrosis (curved arrows). (C) Axial FLAIR image shows peritumoral edema and infiltration. (D) The coronal T2W image with two manually drawn polygonal lines that include the entire peritumoral brain edema (blue line) and tumor (red line); the edema volume is ~equal to the tumor volume. (E) Hemorrhagic lesions (arrowhead) appear markedly hypointense on a conventional T2* GE image. (F) Axial DWI and the corresponding (G) ADC map show a diffusion-restricted lesion within the enhanced tumor. (H) The color-coded CBV map shows higher vascularity in the normal white matter; three ROIs (circles) were placed in the solid tumor component (ROI 1), peritumoral region (ROI 2), and abnormal white matter (ROI 3). The minimum ADC was $0.84x10^{-3}$ mm^2/s in the solid tumor (ADCt), $1.14x10^{-3}$ mm^2/s in the peritumoral edema (ADCe), and $0.62x10^{-3}$ mm^2/s in the normal white matter (ADCn). The rCBV value was 7.62 in the solid tumor (rCBVt), 1.61 in the peritumoral edema (rCBVe), and 1.77 in the normal white matter (rCBVn). GBM, glioblastoma; MRI, magnetic resonance imaging; T1W, contrast-enhanced T1-weighted; FLAIR, fluid-attenuated inversion recovery; ADC, apparent diffusion coefficient; CBV, cerebral blood volume; ROI, circular regions of interest; ADCt, solid tumor ADC value; ADCe, peritumoral edema; ADCn, normal white matter; rCBV, relative cerebral blood volume; rCBVn, normal white matter rCBV value.

Statistical analysis. Statistical analyses were performed using SPSS 20.0 software (IBM Corp.). Qualitative parameters are presented as the number (n) and percentage (%), and quantitative parameters are presented as the mean ± standard

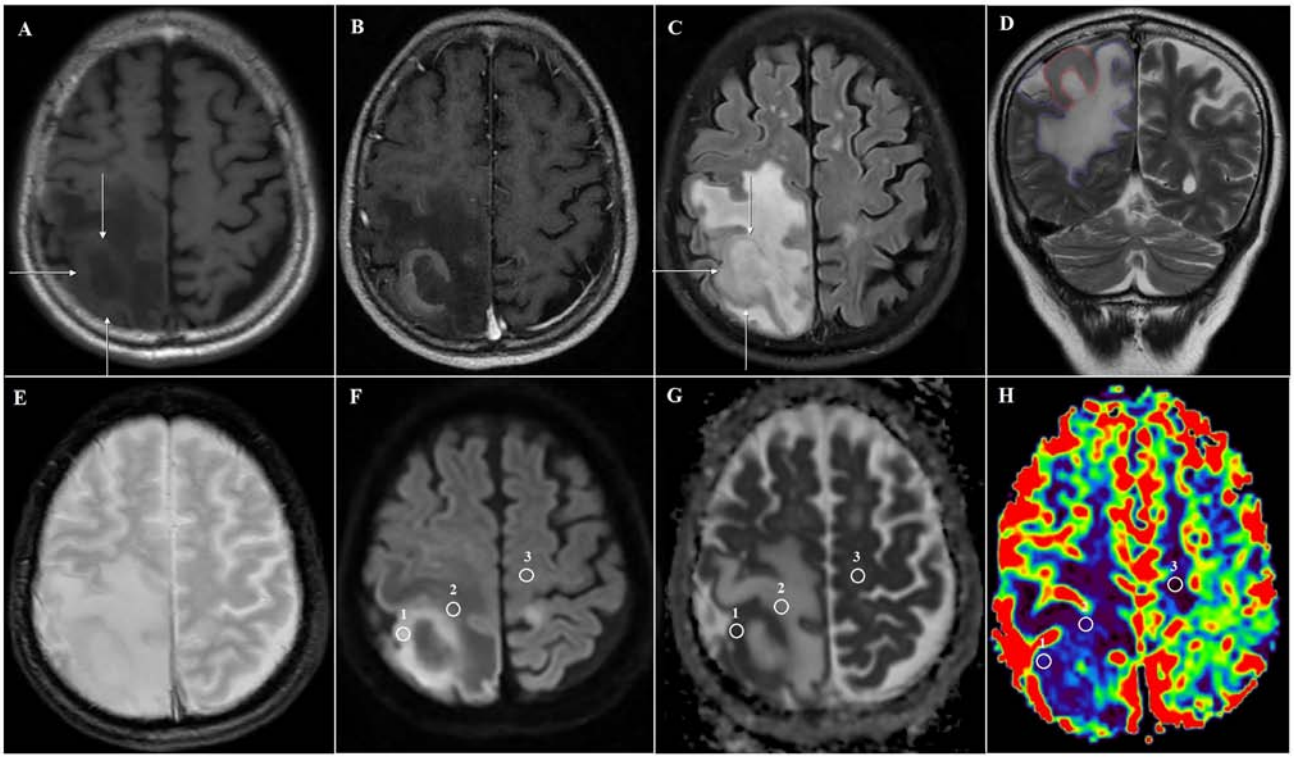

Figure 2. A 70-year-old man with a PCNSL. (A) The MRI shows a mass (straight arrows) in the right parietal lobe. A comparison of (A) pre- and (B) post-contrast T1W images shows a very strong and homogeneous open-ring enhanced tumor. (C) Axial FLAIR and (D) coronal T2W images with two manually drawn polygonal lines that include the entire peritumoral brain edema (blue line) and tumor (red line); the peritumoral volume is greater than the tumor volume. (E) The conventional $T2^*$ GE image shows no intertumoral hemorrhage. (F) Axial DWI and the corresponding (G) ADC map show a diffusion-restricted lesion. (H) The CBV color map shows a lower signal intensity in the tumor than in the normal white matter; three ROIs (circles) were placed in the solid tumor component (ROI 1), peritumoral region (ROI 2), and abnormal white matter (ROI 3). The minimum ADC was $0.63x10^{-3}$ mm^2/s in the solid tumor (ADCt), $1.57x10^{-3}$ mm^2/s in the peritumoral edema (ADCe), and $0.69x10^{-3}$ mm^2/s in the normal white matter (ADCn). The rCBV value was 0.68 in the solid tumor (rCBVt), 0.54 in the peritumoral edema (rCBVe), and 0.37 in the normal white matter (rCBVn). PCNSL, primary central nervous system lymphoma; MRI, magnetic resonance imaging; T1W, contrast-enhanced T1-weighted; FLAIR, fluid-attenuated inversion recovery; DWI, diffusion-weighted; ADC, apparent diffusion coefficient; ADCt, solid tumor ADC value; ADCe, peritumoral edema ADC value; CBV, cerebral blood volume; rCBV, relative cerebral blood volume; rCBVt, solid tumor rCBV value; rCBVe, peritumoral edema rCBV value.

deviation (SD). Before analysis, the normality of each variable's distribution was checked using the Shapiro-Wilk test. Qualitative parameters were compared using the Chi-square (χ^2) test and Fisher's exact test. Non-normally and normally distributed quantitative parameters were compared using the Mann-Whitney test and Student's t-test (also known as unpaired t-test), respectively, in the GBM and PCNSL patient groups. Finally, combinations of significantly different variables were examined to determine the ability of combined parameters to increase diagnostic value. ADC, ADC ratio, rCBV, and rCBV ratio cutoff values for differentiating GBMs and PCNSLs were determined based on a receiver operating characteristic (ROC) curve analysis, with the area under the ROC curve (AUC) calculated as an indicator of overall diagnostic accuracy. All results with $P<0.05$ were considered to indicate a statistically significant difference.

Results

The population of the present study comprised 45 patients (24 men and 21 women) with histologically confirmed tumors, including 27 GBMs (15 men and 12 women) and 18 PCNSLs (nine men and nine women). The mean age was 59.04±11.12 years in the GBM group and 59.50±14.16 years in the PCNSL group. The age and sex distributions did not differ significantly between the GBM and PCNSL groups (Table I). The conventional MRI features of GBMs and PCNSLs are summarized in Table I. Both tumors occurred most often in the supratentorial region. There was no statistically significant difference in their locations. Multiple tumors are more common in patients with GBM (85.2%) than in patients with PCNSL (44.4%). Tumor necrosis was observed in all patients with GBM (100%) but only in three patients with PCNSL (16.7%). All GBMs and PCNSLs demonstrated contrast enhancement of the primary tumor mass. However, heterogeneous enhancement (Fig. 1) was observed in all patients with GBM, contrasting with the homogeneous enhancement (Fig. 2) observed in most patients with PCNSL. PCNSL was enhanced homogenously in 77.8% of cases and heterogeneously in 22.2% of cases. The open-ring sign (Fig. 2B) was present in six (33.3%) patients with PCNSL but in none patient with GBM. Tumor number, tumor enhancement type, tumor necrosis frequency, hemorrhage frequency and open-ring sign frequency differed significantly between GBMs and PCNSLs ($P<0.05$).

The ADC and DWI values in solid tumor and peritumoral edema regions and their ratios to those of normal white matter are summarized for both GBMs and PCNSLs in Table III. DWI

Table III. Diffusion parameter values in GBMs and PCNSLs.

Parameter	Mean ± SD (range) GBM (n=27)	PCNSL (n=18)	P-value
Minimum ADC (10^{-3} mm^2/s)			
ADCt	0.88±0.18 (0.52-1.31)	0.64±0.13 (0.50-1.00)	<0.001
ADCe	1.18±0.23 (0.70-1.61)	1.15±0.25 (0.77-1.57)	0.613[b]
ADCn	0.69±0.66 (0.56-0.90)	0.67±0.68 (0.54-0.78)	0.305[b]
ADC ratio			
ADCt/n	1.28±0.26 (0.81-1.88)	0.96±0.17 (0.73-1.29)	<0.001
ADCe/n	1.72±0.39 (0.98-2.51)	1.71±0.35 (1.13-2.30)	0.900[b]
Mean DWI (10^{-3} mm^2/s)			
DWIt	1.33±0.22 (0.91-1.95)	1.42±0.39 (0.82-2.09)	0.414[b]
DWIe	1.07±0.13 (0.78-1.35)	1.00±0.21 (0.54-1.37)	0.198[b]
DWIn	0.99±0.11 (0.81-1.17)	0.90±0.16 (0.61-1.17)	0.852[b]
DWI ratio			
DWIt/n	1.36±0.25 (1.01-1.99)	1.45±0.32 (0.72-1.98)	0.194[a]
DWIe/n	1.10±0.18 (0.72-1.42)	1.03±0.19 (0.59-1.38)	0.192[b]

GBM, glioblastoma; PCNSL, primary central nervous system lymphoma; a, Mann-Whitney U test; b, Student's t-test; ADC, apparent diffusion coefficient; ADCt, solid tumor ADC value; ADCe, peritumoral edema; ADC value; ADCn, normal white matter ADC value; ADCt/n, the ratio of solid tumor to normal white matter ADC values; ADC e/n, the ratio of peritumoral edema to normal white matter ADC values; DWI, diffusion-weighted imaging; DWIt, solid tumor component DWI value; DWIe, peritumoral edema DWI value; DWIn, normal white matter DWI value; DWIt/n, the ratio of solid tumor to normal white matter DWI values; DWIe/n, the ratio of peritumoral edema to normal white matter DWI values. Two reviewers calculated the ADC and DWI ratios for each lesion.

Table IV. Perfusion parameter values in GBMs and PCNSLs.

Parameter	Mean ± SD (range) GBM (n=27)	PCNSL (n= 8)	P-value
rCBV			
rCBVt	8.41±2.05 (4.43-11.84)	2.34±1.16 (0.56-4.79)	<0.001
rCBVe	2.04±1.07 (0.32-5.24)	1.15±0.76 (0.19-2.77)	0.002[a]
rCBVn	1.90±0.79 (0.67-4.12)	1.92±0.98 (0.37-3.63)	0.954[b]
rCBV ratio			
rCBVt/n	5.02±2.25 (2.36-13.23)	1.49±1.09 (0.44-4.77)	<0.001
rCBVe/n	1.18±0.67 (0.18-3.49)	0.68±0.42 (0.10-1.46)	0.005[a]

GBM, glioblastoma; PCNSL, primary central nervous system lymphoma; a, Mann-Whitney U test; b, Student's t-test; rCBV, relative cerebral blood volume; rCBVt, solid tumor rCBV value; rCBVe, peritumoral edema rCBV value; rCBVn, normal white matter rCBV value; rCBV t/n, the ratio of solid tumor to normal white matter rCBV values; rCBVe/n, the ratio of peritumoral edema to normal white matter rCBV values. Two reviewers calculated the rCBV ratio for each lesion.

values did not differ significantly between GBMs and PCNSLs. The ADC values were higher for GBMs than PCNSLs in the solid tumor (ADCt; P<0.001 but were similar in GBMs and PCNSLs in the peritumoral edema (ADCe; P=0.613). The ratio of ADC values in the peritumoral edema to the normal white matter (ADCe/n) did not differ significantly between GBM and PCNSLs. However, two parameters did differ significantly between GBMs and PCNSLs: the minimum ADC value in the solid tumor (0.88±0.18x10^{-3} mm^2/s in GBMs vs. 0.64±0.13x10^{-3} mm^2/s in PCNSLs; P<0.001) and the ratio of minimum ADC values in the solid tumor to the normal white matter (1.28±0.26 in GBMs vs. 0.96±0.17 in PCNSLs; P<0.001).

The rCBV values in the solid tumor and peritumoral edema regions and their ratios to those of normal white matter are shown for both GBMs and PCNSLs in Table IV. GBMs and PCNSLs differed significantly in rCBV values in the solid tumor (rCBVt; 8.41±2.05 in GBMs vs. 2.34±1.16 in PCNSLs;

Table V. Comparison of univariate and multivariate models for differentiating GBMs and PCNSLs.

	Univariate		Multivariate	
Variable	β	P-value	β	P-value
Quantity	1.972	0.006		
Tumor necrosis	23.400	0.998		
Tumor hemorrhage	3.359	<0.001		
Tumor enhancement	-23.112	0.998		
rCBVt	-0.867	<0.001	-1.021	<0.001
rCBVe	-0.422	0.004	0.417	0.037
rCBVt/n	-0.685	<0.001	0.280	0.165
rCBVe/n	-0.397	0.007	-0.526	0.010
ADCt (10^{-3} mm^2/s)	-0.607	<0.001	-0.305	0.077
ADCt/n	-0.569	<0.001	0.124	0.468

rCBV, relative cerebral blood volume; rCBVt, solid tumor rCBV value; rCBVe, peritumoral edema rCBV value; rCBVn, normal white matter rCBV value; rCBVt/n, the ratio of solid tumor to normal white matter rCBV values; rCBVe/n, the ratio of peritumoral edema to normal white matter rCBV values; ADC, apparent diffusion coefficient; ADCt, solid tumor ADC value; ADCe, peritumoral edema ADC value; ADCn, normal white matter ADC value; ADCt/n, the ratio of solid tumor to normal white matter ADC values; b, standardized beta.

P<0.001) and peritumoral edema (rCBVe; 2.04±1.07 in GBMs vs. 1.15±0.76 in PCNSLs; P=0.002) regions. They also differed significantly in the ratio of mean rCBV values in solid tumors (rCBVt/n; 5.02±2.25 in GBMs vs. 1.49±1.09 in PCNSLs; P<0.001) and peritumoral edema (rCBVe/n; 1.18±0.67 in GBMs vs. 0.68±0.42 in PCNSLs; P=0.005) to normal white matter.

A multivariate logistic regression analysis was performed to assess the joint abilities of different parameters to predict histologic examination results (Table V). The independent variables ADCt, ADCt/n, rCBVt, rCBVe, rCBVt/n and rCBVe/n showed the best discriminative values and were selected for multivariate analysis. While the rCBVt, rCBVe, and rCBVe/n variables were significant in the multivariate regression model, the rCBVt/n, ADCt and ADCt/n variables were not.

As demonstrated in Table VI, the optimal cutoff values, AUCs, sensitivities (Se) and specificities (Sp) of parameters differed significantly between GBMs and PCNSLs. The AUCs differed significantly for ADCt, ADCt/n, rCBVt, rCBVe, rCBVt/n and rCBVe/n (Figs. 3 and 4).

Discussion

Pretreatment characterization and differentiation of malignant brain tumors using MRI remain a challenging problem in everyday practice. While GBMs and PCNSLs differ in numerous respects, their morphological differentiation by MRI is often difficult. The standard treatment for GBMs comprises surgical resection, radiotherapy and chemotherapy, while PCNSLs should not undergo surgical management but only chemotherapy (1,7). In the present study, conventional MRI, DWI and DSC-PWI characteristics were compared between PCNSLs and GBMs, allowing for a more detailed analysis of brain tumors and their *in vivo* differentiation. The present study focused on both the solid tumor and its surrounding brain tissue since they are considered two equally important sources of information necessary for tumor identification. Several significant differences between them were detected.

GBMs are highly vascular due to microvascular proliferation. However, their tumor vasculature characteristics and phenotype were quite different from normal preexisting blood vessels (23). The newly formed vascular networks may fail to mature and prune, leading to increased vessel fragility and hemorrhage risks. Blood flow through the poorly organized and malformed vessels can be chaotic. These factors can lead to areas of persisting or intermittent hypoxia (24). These mechanisms would explain the heterogeneous enhancement pattern with evident necrosis and hemorrhage in almost all patients with GBM in the present study. GBM typically manifested as a solitary infiltrative tumor, and multiple lesions were present in only four cases (14.8%). Conversely, PCNSL lesions presented as homogeneous enhancement lesions, and multiple lesions were present in 10 cases (55.6%). In conventional MRI, it is not possible to distinguish GBMs and PCSNLs based on tumor location and relative peritumoral brain edema to tumor volume since both are generally localized supratentorial, and peritumoral edema degree varies across lesions. Strong-enhancing tumors were observed in almost all GBM and PCNSL cases, and poor-enhancing tumors were observed only in two GBM cases. In the present study, the 'open-ring' enhancement (25) was found in six PCNSL cases (33.3%), characterized by thick and non-uniform rather than thin and uniform brain demyelination.

The MRI findings of the present study for GBMs agree with those previously reported (26,27). However, these findings for PCNSLs are only partially consistent with those reported by Haldorsen *et al* (28). In the present study, 55.6% of PCNSL patients presented with multiple lesions and 27.8% with periventricular lesions. By contrast, Haldorsen *et al* reported multiple lesions in only 35% of PCNSL patients and ventricular wall involvement in 56% of focal lesions. However, Haldorsen *et al* (28) and Malikova *et al* (26) also reported diffuse infiltrative brain affection by PCNSL in 7 and 24.1% of cases, respectively, which were not found in the present study.

The results of the present study were compared with Haldorsen *et al* (28) because their study had a larger sample size than other studies (75 acquired immunodeficiency syndrome-negative PCNSL patients). However, only 52 patients underwent MRI, with the rest examined by computed tomography (CT). Since CT sensitivity is significantly lower than MRI, some lesions may have been missed (no lesions were found in 10 patients). Their study (28) also included patients with immunosuppression therapy (5%), and six patients only had post-steroid treatment imaging available (which may have influenced their imaging findings). Therefore, differences between the results of the present study are partly explainable by differences in patient selection designs.

The results of the present study revealed significant differences in conventional MRI-based tumor number, tumor enhancement type, tumor necrosis frequency, hemorrhage frequency and open-ring sign frequency between GBMs and PCNSLs. Other morphological features (reef sign,

Table VI. ROC analysis results for differentiating PCNSLs and GBMs.

Parameter	AUC[c]	Cutoff value	Sensitivity (%)[a]	Specificity (%)[b]
rCBVt	0.996	4.15	1.00	0.94
rCBVe	0.782	1.10	0.61	0.93
rCBVe/n	0.751	0.54	0.50	0.96
rCBVt + rCBVe	0.998		1.00	0.96
rCBVt + rCBVe/n	1.000		1.00	1.00
rCBVe + rCBVe/n	0.800		0.78	0.78
rCBVt + rCBVe + rCBVe/n	1.000		1.00	1.00

rCBV, relative cerebral blood volume; rCBVt, solid tumor rCBV value; rCBVe, peritumoral edema rCBV value; rCBVe/n, ratio of peritumoral edema to normal white matter rCBV values; a, percentage of correctly classified GBMs; b, percentage of correctly classified PCNSLs; c, area under the receiver operator characteristic curve.

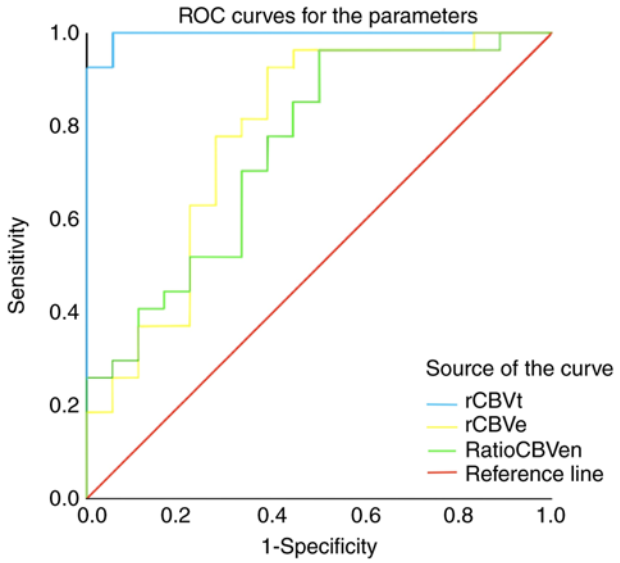

Figure 3. ROC curves of rCBV values for differentiating PCNSLs and GBMs. ROC curves are shown for rCBV values in the solid tumor (rCBVt; blue line) and peritumoral edema (rCBVe; yellow line) regions, and the ratio of peritumoral edema to normal white matter rCBV values (rCBVe/n; green line). The optimal cutoff values for rCBVt, rCBVe, and rCBVe/n were 4.15 (Se=100% and Sp=94%), 1.10 (Se=61% and Sp=93%), and 0.54 (Se=50% and Sp=96%), respectively. The AUCs for rCBVt, rCBVe, and rCBVe/n were 0.996, 0.782, and 0.751, respectively. ROC, receiver operating characteristic; rCBV, relative cerebral blood volume; PCNSL, primary central nervous system lymphoma; GBM, glioblastoma; rCBVt, solid tumor rCBV value; rCBVe, peritumoral edema rCBV value; rCBVe/n, the ratio of peritumoral edema to normal white matter rCBV values.

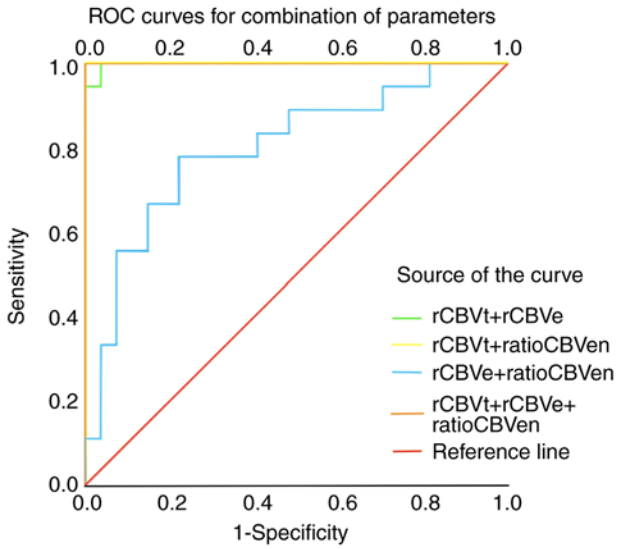

Figure 4. ROC curves of combined parameters for differentiating PCNSLs and GBMs. ROC curves are shown for rCBVt + rCBVe (green line), rCBVt + rCBVe/n (yellow line), rCBVe + rCBVe/n (yellow line), and rCBVt + rCBVe + rCBVe/n (orange line). Their AUCs were 0.998 (Se=100% and Sp=96%), 1.000 (Se=100% and Sp=100%), 0.800 (Se=78% and Sp=78%), and 1.000 (Se=100% and Sp=100%), respectively. ROC, receiver operating characteristic; PCNSL, primary central nervous system lymphoma; GBM, glioblastoma; rCBVt, solid tumor rCBV value; rCBVe, peritumoral edema rCBV value; rCBVe/n, the ratio of peritumoral edema to normal white matter rCBV values; AUC, area under the curve.

peritumoral leukomalacia sign and T2 pseudo-necrosis sign) and signal intensity ratio derived from conventional MRI in distinguishing PCNSL from atypical GBM, were defined in new research by Han *et al* (11). However, unified standard has not established yet. Further prospective studies are required to reliably determine the usefulness of these imaging characteristics. Therefore, it remains difficult to differentiate between GBMs and PCNSLs with conventional MRI alone in clinical practice, particularly in cases with atypical PCNSL with nonhomogeneous enhancement (4/18; 22.2%).

DWI is an advanced imaging method that measures the diffusion properties of water molecules within biological tissues. Therefore, intertumoral ADCs are considered imaging markers of cellularity for various tumors (13). A quantitative ADC analysis showed that the minimum ADC values and ratios were significantly higher in GBMs than in PCNSLs in the solid tumor area ($0.88\pm0.18\times10^{-3}$ mm^2/s vs. $0.64\pm0.13\times10^{-3}$ mm^2/s and 1.28 ± 0.26 vs. 0.96 ± 0.17, respectively) but not in the peritumoral edema area. The lower ADC values of enhancing PCNSL than GBM tumors were due to higher cellularity with a relative reduction in the extracellular space (more restricted diffusion) (13).

While the solid tumor results of th present study are consistent with previous studies, the ADC values are slightly higher. Yamashita *et al* (29) reported minimum ADC values for GBMs and PCNSLs of $0.78\pm0.19\times10^{-3}$

and $0.61\pm0.13x10^{-3}$ mm^2/s, respectively. Lee *et al* (3) reported minimum ADC values for PCNSLs and GBMs of $0.595\pm0.228x10^{-3}$ and $0.737\pm0.162x10^{-3}$ mm^2/s, respectively, and minimum ADC ratios for PCNSLs and GBMs of 0.87±0.26 and 1.14±0.29, respectively. Feng *et al* (16) reported minimum ADC values for PCNSLs and GBMs of $0.68\pm0.10x10^{-3}$ and $0.77\pm0.07x10^{-3}$ mm^2/s, respectively, and relative ADC for PCNSLs and GBMs of 1.13±0.12 and 1.32±0.19, respectively. In contrast to the present study, a previous study of 20 patients by Bao *et al* (17) showed that although ADC parameters were larger in GBM compared with those in PCNSL, but these differences were not statistically significant. This difference could be explained by the whole-tumor histogram analysis which be affected by the tumor size (larger tumors will have a greater impact on total tumor diffusion metrics compared with smaller tumors). Furthermore, these studies (3,16,17,29) did not evaluated the peritumoral edema.

The present findings on the utility of peritumoral zone ADC values are consistent with Server *et al* (30) but inconsistent with Martín-Noguerol *et al* (31), who found subtle differences in ADC values between the infiltrating edema of GBMs and the vasogenic edema of PCNSLs. Differences between their and the present results may be explained by both infiltrating edema and pure vasogenic edema regions usually showing high ADC values (30), and there was not a sufficient disparity to quantify. Furthermore, a radiologic-pathologic study by Koeller *et al* (32) reported diffuse microscopic tumor infiltrating in peritumoral edema of PCNSLs. Unfortunately, an intraoperative biopsy was not usually performed in the peritumoral edema area for PCNSLs obtained to pathologically confirm the presence of infiltrative tumor cells (21).

To the best of our knowledge, this is the first study comparing quantitative DWI in the solid tumor and peritumoral edema between GBM and PCNSLs. According to the authors' observations, they do not differ significantly in their DWI values.

MRI perfusion imaging can visualize the nutritive delivery of arterial blood to the capillary bed in tumors. Angiogenesis is a fundamental cancer hallmark, which varies among tumor types (24). Unlike PCNSLs, which show an angiocentric growth pattern with cancer cells clustering around preexisting brain vessels, one hallmark of GBMs is extensive neovascularization (13). This characteristic is usually used to explain their differences in rCBV, with higher values in patients with GBMs, which is consistent with the findings of the present study and several other studies (13,15). The solid tumor results of the present study demonstrated significant differences in rCBVt values and rCBVt/n ratios between GBMs and PCNSLs. The rCBVt values and rCBVt/n ratios were 2.34±1.16 and 1.49±1.09 for patients with PCNSLs and 8.41±2.05 and 5.02±2.25 for patients with GBMs. The aforementioned values were substantially higher than those of Neska-Matuszewska *et al* (15), who reported rCBVt values of 0.80±0.35 for PCNSLs and 3.10±1.50 for GBMs, and Feng *et al* (16), who reported rCBVt values of 2.17±0.67 for PCNSLs and 2.38±0.62 for GBMs. The markedly higher rCBV values of the present study may be explained by differences in DSC-PWI measurement methods.

The next step in the present study was to evaluate a non-enhancing peritumoral region to distinguish GBMs from PCNSLs. Peritumoral edema in PCNSLs induce purely vasogenic edema whereas GBMs predominantly contains infiltrating non-contrast-enhancing tumor (infiltrating edema) due to preservation of the blood-brain barrier, usually best visualized on T2W FLAIR imaging (31). Therefore, some authors have proposed evaluating non-enhancing peripheral lesion areas to increase diagnostic accuracy (33). The present study revealed significantly increased rCBVe values and rCBVe/n ratios for GBMs, reflecting neoplastic infiltration into the surrounding peritumoral zone. In Table IV, it is shown that the rCBVe values and rCBVe/n ratios for peritumoral edema areas were 1.15±0.76 and 0.68±0.42 for patients with PCNSLs and 2.04±1.07 and 1.18±0.67 for patients with GBMs. The results are consistent with those of a previous study (15).

The present study evaluated the multiparametric diagnostic performance of DWI and DSC-PWI to facilitate the preoperative differentiation of PCNSL and GBM which are similar to several other studies (15,16,18-20). To differentiate GBMs and PCNSLs, it was suggested a cutoff value of 4.15 for rCBVt, which had 100% Se and 94% Sp with an excellent AUC of 0.996. As it was revealed in the present study, peritumoral zone parameters with the highest accuracies in differentiating GBMs and PCNSLs were the rCBVe value followed by the rCBVe/n ratio with cutoff values of 1.10 (Se=61% and Sp=93%) and 0.54 (Se=50% and Sp=96%), respectively. Since rCBVt achieved the highest accuracy in distinguishing GBMs and PCNSLs, it was suggested to focus on measuring this parameter in clinical practice. Individual parameters had a limited role in differentiating GBMs and PCNSLs. A multiparametric model comprising rCBVt, rCBVe, and rCBVe/n significantly improved the ability to differentiate PCNSLs and GBMs compared with the univariate models (Table IV). While the AUCs for rCBVe and rCBVe/n for differentiating GBMs and PCLs were only 0.782 and 0.751, respectively, an improved AUC (0.80) was obtained by combining rCBVe and rCBVe/n. Furthermore, a perfect AUC (1.00) with 100% Se and 100% Sp for differentiating GBMs and PCNSLs was obtained by combining either rCBVt with rCBVe/n or all three parameters (rCBVt + rCBVe + rCBVe/n). However, adding the third imaging parameter (three-variable model) was not significantly superior to the two-variable model.

The present study had certain limitations that should be noted. Firstly, population was small, with some patients excluded because they had no MRI sequences. Nevertheless, a significant difference in MRI characteristics (ADC value, ADC ratio, rCBV value, and rCBV ratio) was identified between PCNSLs and GBMs, consistent with previous studies. Second, PCNSLs occurred less frequently than GBMs. Third, the present study was retrospective. A pooling analysis of retrospective studies could have increased diagnostic performance. Therefore, further prospective studies on the diagnostic performance of DWI and DSC-PWI are needed. Fourth, a unified DWI-based methodology should be established since differences in imaging parameters, field strengths, and post-processing software could all lead to discrepancies in ADC measurement.

The results of the present study indicated that the most important parameter differentiating GBMs and PCNSLs combines rCBVt with rCBVe/n. From a practical perspective, evaluating ADCt could be followed by assessing rCBV values since this parameter is easily accessible on workstations from

all vendors. In addition, the accurate determination of GBM extensions could create numerous opportunities associated with vascular targeting during cancer therapy, with advanced MRI sequences, such as DSC-PWI, suitable for this purpose with acceptable results.

Acknowledgements

Not applicable.

Funding

No funding was received.

Availability of data and materials

The datasets generated and/or analysed during the current study are not publicly available due to privacy concerns but are available from the corresponding author on reasonable request.

Authors' contributions

NNA and NDH confirm the authenticity of all the raw data. NDH, NNA, NDM, DKH and NMD contributed to the conception of the study. NNA, NDH and NMD were responsible for writing the original draft, reviewing and editing the manuscript. NNA and NMD were responsible for critical revision of the manuscript and the analysis and interpretation of the data. All authors read and approved the final version of the manuscript.

Ethics approval and consent to participate

The present study was approved (approval no. 4096/QD-ĐHYHN; date: September 30, 2022) by Hanoi Medical University Institutional Ethical Review Board (Hanoi, Vietnam) and conducted according to the ethical standards of the 1964 Declaration of Helsinki and its later amendments. Informed consent was waived for the study's retrospective nature, and the analysis used anonymous clinical data.

Patient consent for publication

Not applicable.

Competing interests

The authors declare that they have no competing interests.

References

1. Hanif F, Muzaffar K, Perveen K, Malhi SM and Simjee SU: Glioblastoma multiforme: A review of its epidemiology and pathogenesis through clinical presentation and treatment. Asian Pac J Cancer Prev 18: 3-9, 2017.
2. Salacz ME, Watson KR and Schomas DA: Glioblastoma: Part I. Current state of affairs. Mo Med 108: 187-194, 2011.
3. Lee SC, Moon WJ, Choi JW, Roh HG, Bak SH, Yi JG, Yim YJ and Chung EC: Differentitation between primary central nervous system lymphoma and glioblastoma: Added value of quantitative analysis of CT attenuation and apparent diffusion coefficient. J Korean Soc Magn Reson Med 16: 226-235, 2012.
4. Tang YZ, Booth TC, Bhogal P, Malhotra A and Wilhelm T: Imaging of primary central nervous system lymphoma. Clin Radiol 66: 768-777, 2011.
5. Konjević G, Jurisić V, Banićevic B and Spuzić I: The difference in NK-cell activity between patients with non-Hodgkin's lymphomas and Hodgkin's disease. Br J Haematol 104: 144-151, 1999.
6. Jurišić V, Konjević G, Banićević B, Duricić B and Spuzić I: Different alterations in lactate dehydrogenase activity and profile of peripheral blood mononuclear cells in Hodgkin's and non-Hodgkin's lymphomas. Eur J Haematol 64: 259-266, 2000.
7. Han CH and Batchelor TT: Diagnosis and management of primary central nervous system lymphoma. Cancer 123: 4314-4324, 2017.
8. Urbańska K, Sokołowska J, Szmidt M and Sysa P: Glioblastoma multiforme-an overview. Contemp Oncol (Pozn) 18: 307-312, 2014.
9. Mizobuchi Y, Nakajima K, Fujihara T, Matsuzaki K, Mure H, Nagahiro S and Takagi Y: The risk of hemorrhage in stereotactic biopsy for brain tumors. J Med Invest 66: 314-318, 2019.
10. Vaquero J, Martínez R and Manrique M: Stereotactic biopsy for brain tumors: Is it always necessary? Surg Neurol 53: 432-437, 2000.
11. Han Y, Wang ZJ, Li WH, Yang Y, Zhang J, Yang XB, Zuo L, Xiao G, Wang SZ, Yan LF and Cui GB: Differentiation between primary central nervous system lymphoma and atypical glioblastoma based on MRI morphological feature and signal intensity ratio: A retrospective multicenter study. Front Oncol 12: 811197, 2022.
12. Kickingereder P, Wiestler B, Sahm F, Heiland S, Roethke M, Schlemmer HP, Wick W, Bendszus M and Radbruch A: Primary central nervous system lymphoma and atypical glioblastoma: Multiparametric differentiation by using diffusion-, perfusion-, and susceptibility-weighted MR imaging. Radiology 272: 843-850, 2014.
13. Kono K, Inoue Y, Nakayama K, Shakudo M, Morino M, Ohata K, Wakasa K and Yamada R: The role of diffusion-weighted imaging in patients with brain tumors. AJNR Am J Neuroradiol 22: 1081-1088, 2001.
14. Aronen HJ, Gazit IE, Louis DN, Buchbinder BR, Pardo FS, Weisskoff RM, Harsh GR, Cosgrove GR, Halpern EF and Hochberg FH: Cerebral blood volume maps of gliomas: Comparison with tumor grade and histologic findings. Radiology 191: 41-51, 1994.
15. Neska-Matuszewska M, Bladowska J, Sąsiadek M and Zimny A: Differentiation of glioblastoma multiforme, metastases and primary central nervous system lymphomas using multiparametric perfusion and diffusion MR imaging of a tumor core and a peritumoral zone-Searching for a practical approach. PLoS One 13: e0191341, 2018.
16. Feng A, Li L, Huang T, Li S, He N, Huang L, Zeng M and Lyu J: Differentiating glioblastoma from primary central nervous system lymphoma of atypical manifestation using multiparametric magnetic resonance imaging: A comparative study. Heliyon 9: e15150, 2023.
17. Bao S, Watanabe Y, Takahashi H, Tanaka H, Arisawa A, Matsuo C, Wu R, Fujimoto Y and Tomiyama N: Differentiating between glioblastoma and primary CNS lymphoma using combined whole-tumor histogram analysis of the normalized cerebral blood volume and the apparent diffusion coefficient. Magn Reson Med Sci 18: 53-61, 2019.
18. Makino K, Hirai T, Nakamura H, Kuroda JI, Shinojima N, Uetani H, Kitajima M and Yano S: Differentiating between primary central nervous system lymphomas and glioblastomas: Combined use of perfusion-weighted and diffusion-weighted magnetic resonance imaging. World Neurosurg 112: e1-e6, 2018.
19. Nakajima S, Okada T, Yamamoto A, Kanagaki M, Fushimi Y, Okada T, Arakawa Y, Takagi Y, Miyamoto S and Togashi K: Differentiation between primary central nervous system lymphoma and glioblastoma: A comparative study of parameters derived from dynamic susceptibility contrast-enhanced perfusion-weighted MRI. Clin Radiol 70: 1393-1399, 2015.
20. Abul-Kasim K, Maly P, Strömbeck A, Svensson J and Sundgren PC: Perfusion weighted MR imaging may differentiate primary CNS lymphoma from other homogeneously enhancing brain tumors. Neuroradiol J 21: 637-644, 2008.
21. Ko CC, Tai MH, Li CF, Chen TY, Chen JH, Shu G, Kuo YT and Lee YC: Differentiation between glioblastoma multiforme and primary cerebral lymphoma: Additional benefits of quantitative diffusion-weighted MR imaging. PLoS One 11: e0162565, 2016.
22. Osborn AG, Louis DN, Poussaint TY, Linscott LL and Salzman KL: The 2021 world health organization classification of tumors of the central nervous system: What neuroradiologists need to know. AJNR Am J Neuroradiol 43: 928-937, 2022.

23. Das S and Marsden PA: Angiogenesis in glioblastoma. N Engl J Med 369: 1561-1563, 2013.
24. Lugano R, Ramachandran M and Dimberg A: Tumor angiogenesis: Causes, consequences, challenges and opportunities. Cell Mol Life Sci 77: 1745-1770, 2020.
25. Zhang D, Hu LB, Henning TD, Ravarani EM, Zou LG, Feng XY, Wang WX and Wen L: MRI findings of primary CNS lymphoma in 26 immunocompetent patients. Korean J Radiol 11: 269-277, 2010.
26. Malikova H, Koubska E, Weichet J, Klener J, Rulseh A, Liscak R and Vojtech Z: Can morphological MRI differentiate between primary central nervous system lymphoma and glioblastoma? Cancer Imaging 16: 40, 2016.
27. Osborn AG, Salzman KL and Jhaveri MD (eds): Diagnostic Imaging Brain. 3rd edition. Elsevier, Philadelphia, PA, 2016.
28. Haldorsen IS, Kråkenes J, Krossnes BK, Mella O and Espeland A: CT and MR imaging features of primary central nervous system lymphoma in Norway, 1989-2003. AJNR Am J Neuroradiol 30: 744-751, 2009.
29. Yamashita K, Yoshiura T, Hiwatashi A, Togao O, Yoshimoto K, Suzuki SO, Abe K, Kikuchi K, Maruoka Y, Mizoguchi M, *et al*: Differentiating primary CNS lymphoma from glioblastoma multiforme: assessment using arterial spin labeling, diffusion-weighted imaging, and ^{18}F-fluorodeoxyglucose positron emission tomography. Neuroradiology 55: 135-143, 2013.
30. Server A, Kulle B, Maehlen J, Josefsen R, Schellhorn T, Kumar T, Langberg CW and Nakstad PH: Quantitative apparent diffusion coefficients in the characterization of brain tumors and associated peritumoral edema. Acta Radiol 50: 682-689, 2009.
31. Martín-Noguerol T, Mohan S, Santos-Armentia E, Cabrera-Zubizarreta A and Luna A: Advanced MRI assessment of non-enhancing peritumoral signal abnormality in brain lesions. Eur J Radiol 143: 109900, 2021.
32. Koeller KK, Smirniotopoulos JG and Jones RV: Primary central nervous system lymphoma: Radiologic-pathologic correlation. Radiographics 17: 1497-1526, 1997.
33. Lasocki A and Gaillard F: Non-contrast-enhancing tumor: A new frontier in glioblastoma research. AJNR Am J Neuroradiol 40: 758-765, 2019.